Subgrid-scale stress modelling based on the square of the velocity gradient tensor

By F. Nicoud and F. Ducros

CERFACS - Centre Européen de Recherche et de Formation Avancée en Calcul Scientifique

42, Avenue Gaspard Coriolis, 31057 Toulouse cedex, France

tel: (33) 561 19 30 46 fax:(33) 561 19 30 00

email: nicoud@cerfacs.fr

Flow, Turbulence and Combustion, April 1999

Abstract

A new subgrid scale model is proposed for Large Eddy Simulations in complex geometries. This model which is based on the square of the velocity gradient tensor accounts for the effects of both the strain and the rotation rate of the smallest resolved turbulent fluctuations. Moreover it recovers the proper y^3 near-wall scaling for the eddy viscosity without requiring dynamic procedure. It is also shown from a periodic turbulent pipe flow computation that the model can handle transition.

1 Introduction

In the last twenty years, Direct Numerical Simulations (DNS) have modified the way turbulent flows are studied. By providing new tools to investigate the instantaneous three-dimensional structure of turbulent flows, DNS has allowed significant advances both in the understanding and the modeling of turbulence. However, DNS are restricted to low Reynolds numbers so that Large Eddy Simulations (LES) are preferred in practical applications. In the LES approach, scales smaller than the grid size are not resolved but accounted for through the subgrid scale tensor T_{ij} given by

$$T_{ij} = \overline{u}_i \overline{u}_j - \overline{u_i u_j},$$

where the overbar denotes an appropriately chosen low-pass filter and incompressibility is assumed. Most subgrid scale models are based on an eddy-viscosity assumption to model the subgrid scale tensor:

$$T_{ij} - \frac{1}{3} T_{kk} \delta_{ij} = 2\nu_t \overline{S}_{ij},$$

where

$$\overline{S}_{ij} = \frac{1}{2} \left(\frac{\partial \overline{u}_i}{\partial x_j} + \frac{\partial \overline{u}_j}{\partial x_i} \right)$$

is the deformation tensor of the resolved field. In Smagorinsky's model, the eddy-viscosity is assumed to be proportional to the subgrid characteristic length scale Δ and to a characteristic turbulent velocity taken as the local strain rate $\left|\overline{S}\right|$:

$$\nu_t = (C_s \Delta)^2 \left|\overline{S}\right|, \qquad \left|\overline{S}\right| = \sqrt{2\overline{S}_{ij}\overline{S}_{ij}}. \tag{1}$$

Following Lilly [1] , the constant C_s may be obtained by assuming that the cut-off wave number $k_c = \pi/\Delta$ lies within a $k^{-5/3}$ Kolmogorov cascade for the energy spectrum $E(k) = C_K \epsilon^{2/3} k^{-5/3}$ and requiring that the ensemble-averaged subgrid dissipation is identical to ϵ. An approximate value for the constant is then:

$$C_s = \frac{1}{\pi}\left(\frac{3C_K}{2}\right)^{-3/4}.$$

For a Kolmogorov constant of $C_K \simeq 1.4$, this yields $C_s \simeq 0.18$.

Note that the choice of the local strain rate to define the velocity scale at the cut-off is quite arbitrary. If one considers that the velocity gradient tensor is a good candidate to describe the turbulent fluctuations, other invariants based on this tensor could be used for defining the velocity scale needed for the eddy-viscosity ν_t. The aim of this latter quantity is to mimic the energy transfer from the resolved scales to the subgrid ones through the subgrid dissipation (which is proportional to ν_t). Thus by defining the eddy-viscosity from the local strain rate, one relates the subgrid dissipation to the strain rate of the smallest resolved scales of motion. This choice is not in agreement with the results from Wray and Hunt [2] on the kinematic and dynamic properties of the turbulent structures. From direct numerical simulations of isotropic turbulence, these authors have shown that energy is concentrated in the streams and energy dissipation in eddies and convergence zones. Clearly the classical Smagorinsky formulation does not account for the contribution of the former which are regions where vorticity dominates irrotational strain. On the other hand the dominant deformation in convergence zones is irrotational strain so that

the strain rate could be a good measure of their dissipative activity. Thus a better subgrid scale model should be based on both $\left|\overline{S}\right|$ and the rotational rate. This requirement is met by the structure function model [3] which reads:

$$\nu_t = \beta C_K^{-3/2} \Delta \sqrt{\overline{F}_2}, \tag{2}$$

where $\overline{F}_2$ is the second order velocity structure function of the filtered field:

$$\overline{F}_2(\vec{x}, \Delta) = \left\langle ||\overline{\vec{u}}(\vec{x}, t) - \overline{\vec{u}}(\vec{x} + \vec{r}, t)||^2 \right\rangle_{||\vec{r}||=\Delta},$$

and β is a constant which can be fixed from energetic considerations. Very good results have been obtained with this model for isotropic homogeneous turbulence [4]. Other formulations have been proposed to assess the subgrid scale stress, based on the local strain and rotation rate tensors and products of them[5].

A second difficulty in LES is the behaviour of the eddy-viscosity near a wall. By construction, the Smagorinsky model gives a non-zero value of ν_t as soon as a velocity gradient exists. Near a wall, however, all turbulent fluctuations are damped so that ν_t should be zero. To this end, the Van Driest [6] exponential damping function $1 - \exp(-y^+/A^+)$ with $A^+ = 25$, was used widely in early LES studies. This standard modification improves the results dramatically and is very easy to implement for simple geometries. However, it is an *ad hoc* modification based on the distance to the wall. This is difficult to implement in the general case for complex geometries. It also requires the use of a smaller value for the Smagorinsky constant ($C_s = 0.1$) in order to sustain turbulence in a channel flow [7]. Note also that depending on the damping function used it may not produce the proper near-wall scaling for the eddy-viscosity. The above-mentioned

Van Driest damping produces $\nu_t = O(y^2)$ instead of $O(y^3)$. Neither is the classical structure function model well-suited for wall bounded flows. Indeed, the $\overline{F}_2$ function is of order O(1) near a wall when computed as a local statistical average of square velocity differences between the current position and the six closest surrounding points on the (structured) computational grid. A possible remedy for this is to compute $\overline{F}_2$ by using only the four closest points parallel to a given plane. If the plane is parallel to the wall, $\overline{F}_2$ is of order O(y) and better results are obtained in a boundary layer [8, 9]. Another way to produce zero eddy-viscosity at the wall is to modify the constant of the model (C_s for the Smagorinsky model) in such a way as to enforce $C_s \simeq 0$ when turbulence activity is reduced. This is done dynamically by the procedure proposed by Germano et al. [10] , in which the variable $C = C_s^2$ appears in five independent equations. Most of the time, this undeterminacy is dealt with by choosing the value of C (as a function of space and time) that best satisfies the over-determinated system stemming from the Germano identity [1] . However, this procedure often leads to a significant fraction of negative values for C, and thus may generate numerical instabilities. A common remedy involves averaging C over space but this procedure is restricted to simple geometries since the existence of direction of flow homogeneity is required (as in a channel flow).

A third difficulty in modern LES is the necessity to handle complex geometries without direction of flow homogeneity and/or with unstructured numerical methods. The Smagorinsky model is quite well adapted to these configurations since only *local* gradients are involved in the computation of the eddy-viscosity. A Lagrangian version of its dynamic form has been proposed by Meneveau et al.[11] to allow the computation of complex configurations without direction of flow homogeneity. Very good results have been obtained with this formulation which requires the

resolution of two other transport equations [11]. The dynamic localization models (constrained or with a transport equation for the kinetic energy) proposed by Ghosal et al. [12] are in principle applicable to general inhomogeneous flows and do not require spatial averaging. Still, the dynamic procedure is based on the energy transfer between the resolved field and low-pass filtered field. Practically, the width of the filter is Δ for the first field and $\gamma\Delta$ for the second ($\gamma \simeq 2$ is often used). In simple geometries, the filtering operations can be performed very precisely in Fourier space but defining a test filter of width 2Δ in complex geometries may prove to be an issue [13].

All the above discussed models may be written in the generic form:

$$\nu_t = C_m \Delta^2 \overline{OP}(\vec{x}, t), \tag{3}$$

where C_m is the constant [1] of the model, Δ is the subgrid characteristic length scale (in practice the size of the mesh) and OP is an operator of space and time, homogeneous to a frequency, and defined from the resolved fields. In this paper we propose to define a new operator $\overline{OP}$ with the four following major properties:

- it should be invariant to any coordinate translation or rotation,
- it can be easily assessed on any kind of computational grid,
- it is a function of both the strain and the rotation rates, in agreement with recent findings concerning the contribution of the turbulent structures to the global dissipation,
- it goes naturally to zero at the wall so that neither damping function nor dynamic procedure are needed to reproduce the effect of the no-slip condition.

[1] which can be adapted in a dynamic way

The resulting WALE (Wall-Adapting Local Eddy-viscosity) model is based on a tensor invariant and reproduces the proper scaling at the wall ($\nu_t = O(y^3)$). It is also well-suited for LES in complex geometries with structured or unstructured methods because no explicit filtering is needed and only local information is required to build the eddy-viscosity. Finally, it is sensitive to both the strain and the rotation rate of the small turbulent structures. Although the dynamic procedure could also be applied to the WALE model, C_m is considered here as a true constant, assessed from the canonic case of isotropic homogeneous turbulence. The model is defined in section 2 and used for the case of the pipe flow in section 3.

2 Eddy-viscosity models

The filtered Smagorinsky model [14, 15] will be used as a reference in section 3, together with the classical Smagorinsky formulation. It is briefly presented in the following subsection for clarity. More details about the filtered approach can be found in Ducros et al. [9]. The WALE model is then presented with some details.

2.1 Filtered Smagorinsky model

This is a Smagorinsky model defined on high-pass filtered velocity fields, following to previous works concerning the filtered structure function model [9, 4]:

$$\nu_t = (C_2\Delta)^2\sqrt{2HP(\overline{S_{ij}})HP(\overline{S_{ij}})} \quad , \tag{4}$$

where $HP(\overline{S}_{ij})$ stands for the resolved strain rate defined on high-pass filtered velocity fields. Here the high-pass filtered velocity fields are obtained using an estimation of the fourth-order derivatives of conserved variables [16]. As in Ducros et al. [9], the transfer function of the high-pass filter is numerically evaluated, which gives:

$$\frac{E_{HP}(k)}{E(k)} = a\left(\frac{k}{k_c}\right)^b \quad , \tag{5}$$

where $E_{HP}(k)$ stands for the energy spectrum of the filtered field and $a \approx 0.35$ and $b \approx 6.66$ are two constants determined numerically. The constant C_2 is then determined using the same method as C_s, *ie* by prescribing:

$$\epsilon = \langle 2\nu_t\overline{S_{ij}}\ \overline{S_{ij}}\rangle \quad , \tag{6}$$

and assuming

$$\langle 2HP(\overline{S_{ij}})HP(\overline{S_{ij}})\rangle = 2\int_0^{k_c} k^2 E_{HP}(k)dk \quad , \tag{7}$$

which gives

$$C_2 = \left(\frac{2}{3}C_k^{-3/2}\sqrt{\frac{3b+4}{6a}}\frac{1}{\pi^2}\right)^{1/2} \approx 0.37 \quad . \tag{8}$$

The filtered Smagorinsky model was used to compute a turbulent pipe flow with a hybrid mesh [14, 15] and the results were shown to be consistent with both previous numerical and experimental studies [17].

2.2 The WALE model

Choice of the Invariant

In LES, the eddy-viscosity ν_t must not change when the frame of reference is changed, thus the operator $\overline{OP}$ must be based on the invariants of a tensor $\overline{\tau}_{i,..,j}$ which should be representative of the turbulent activity. Clearly, the velocity gradient tensor $\overline{g}_{ij} = \partial\overline{u}_i/\partial x_j$ is a good candidate to represent the velocity fluctuations at the length scale Δ. The Smagorinsky model is based on the second invariant of the symmetric part $\overline{S}_{ij}$ of this tensor. Recall that two major drawbacks are associated with this choice:

- this invariant is only related to the strain rate of the turbulent structure but not to their rotation rate,
- this invariant is of order $O(1)$ near a wall.

Let us first consider the second point. If a flat plate is placed at $y = 0$, the resolved part of the velocity field can be expanded, in the limit $y \simeq 0$ and $y > 0$, as follows:

$$\begin{aligned} \overline{u} &= u_1 y + u_2 y^2 + O(y^3), \\ \overline{v} &= v_2 y^2 + O(y^3), \\ \overline{w} &= w_1 y + w_2 y^2 + O(y^3), \end{aligned} \tag{9}$$

where u_1, u_2, v_2, w_1 and w_2 are function of space (x, z) and time and v_1 is zero from the kinematic condition $\partial \overline{u}_i / \partial x_i = 0$ which holds for incompressible flows. This means that the first invariant of the velocity gradient tensor $\overline{g}$ is zero as well as the first invariant of its symmetric part ($\overline{g}_{ii} = \overline{S}_{ii}$). Also, in case of homogeneous incompressible flow, the ensemble-averaged second invariant of $\overline{g}_{ij}$ is identically zero (since $\overline{g}_{ii} = 0$ and $\left\langle \overline{g}_{ij} \overline{g}_{ji} \right\rangle$=0, <> denoting the ensemble average). On the other hand, the second invariant of $\overline{S}$ is $-\frac{1}{2}\overline{S}_{ij}\overline{S}_{ij}$, strongly related to the spatial operator used in the Smagorinsky model $\overline{OP} = \sqrt{2\overline{S}_{ij}\overline{S}_{ij}}$. In the limit $y \simeq 0$, it is obvious to show from relations 9 that this quantity remains finite (of order $O(1)$). The same kind of results may be obtained for the third invariant of $\overline{g}_{ij}$ and $\overline{S}_{ij}$. Thus, all the operators one can build from these tensors lead to the non-physical behaviour $\nu_t = O(1)$ at the wall.

A simple way to build a better operator is to consider the traceless symmetric part of the square of the velocity gradient tensor:

$$\mathcal{S}^d_{ij} = \frac{1}{2}\left(\overline{g}^2_{ij} + \overline{g}^2_{ji}\right) - \frac{1}{3}\delta_{ij}\overline{g}^2_{kk}, \tag{10}$$

where $\overline{g}^2_{ij} = \overline{g}_{ik}\overline{g}_{kj}$ and δ_{ij} is the Kronecker symbol.

Let us note $\overline{\Omega}$ the anti-symmetric part of $\overline{g}$:

$$\overline{\Omega}_{ij} = \frac{1}{2}\left(\frac{\partial \overline{u}_i}{\partial x_j} - \frac{\partial \overline{u}_j}{\partial x_i}\right)$$

The tensor defined by the relation 10 can be rewritten in terms of $\overline{S}$ and $\overline{\Omega}$. One obtains:

$$\mathcal{S}_{ij}^d = \overline{S}_{ik}\overline{S}_{kj} + \overline{\Omega}_{ik}\overline{\Omega}_{kj} - \frac{1}{3}\delta_{ij}\left[\overline{S}_{mn}\overline{S}_{mn} - \overline{\Omega}_{mn}\overline{\Omega}_{mn}\right], \tag{11}$$

By construction, the trace of $\mathcal{S}^d$ is zero and its second invariant remains finite and proportional to $\mathcal{S}_{ij}^d\mathcal{S}_{ij}^d$. By using relation 11 and making use of the Cayley-Hamilton theorem of linear algebra, this quantity can be developed as (assuming incompressibility):

$$\mathcal{S}_{ij}^d\mathcal{S}_{ij}^d = \frac{1}{6}\left(S^2S^2 + \Omega^2\Omega^2\right) + \frac{2}{3}S^2\Omega^2 + 2IV_{S\Omega}, \tag{12}$$

with the notations:

$$S^2 = \overline{S}_{ij}\overline{S}_{ij}, \qquad \Omega^2 = \overline{\Omega}_{ij}\overline{\Omega}_{ij}, \qquad IV_{S\Omega} = \overline{S}_{ik}\overline{S}_{kj}\overline{\Omega}_{jl}\overline{\Omega}_{li}$$

From this last relation, a LES model based on $\mathcal{S}_{ij}^d\mathcal{S}_{ij}^d$ will detect turbulence structures with either (large) strain rate, rotation rate or both. In the case of pure shear (e.g. $\overline{g}_{ij} = 0$ except $\overline{g}_{12}$), it yields $S^2 = \Omega^2 = 4\overline{S}_{12}$ and $IV_{S\Omega} = -\frac{1}{2}S^2S^2$ so that the considered invariant is zero. This point is in agreement with the fact that the shear zones contribute to energy dissipation to a smaller extent than convergence zones and eddies [2]. Moreover this means that almost no eddy-viscosity would be produced in the case of a wall-bounded laminar flow (Poiseuille flow). Thus the amount of turbulent diffusion would be negligible in such a case and the development of linearly unstable waves would be possible. This is a great advantage over the Smagorinsky model which is unable to reproduce the laminar to turbulent transition of such flow because the invariant $\overline{S}_{ij}\overline{S}_{ij}$ is large in the case of pure shear. It is shown in section 3 that the WALE model based on the $\mathcal{S}_{ij}^d\mathcal{S}_{ij}^d$ invariant can handle the transitional pipe flow.

Wall Behaviour and Scaling

In the limit $y \simeq 0$, it can be shown from relations 9 that $\mathcal{S}_{ij}^d \mathcal{S}_{ij}^d$ behaves like y^2. Thus a simple way to build a spatial operator $\overline{OP}$ which behaves like y^3 near a wall is to take $\overline{OP}$ proportional to $\overline{OP}_1 = \left(\mathcal{S}_{ij}^d \mathcal{S}_{ij}^d\right)^{3/2}$. Since $\overline{g}$ has the dimension of frequency, $\overline{OP}_1$ has the dimension of frequency to the power 6 and must be scaled before being used in the subgrid scale model formulation 3. Of course, the scaling must be of O(1) near a wall in order to keep the y^3 behaviour of the whole operator. The first possible scale could be $(\overline{S}_{ij}\overline{S}_{ij})^{5/2}$ because it has the dimension of frequency to the power 5 and it is O(1) near a wall. However the ratio $\overline{OP}_1/(\overline{S}_{ij}\overline{S}_{ij})^{5/2}$ is not well conditioned numerically since the denominator can (locally) tend to zero while $\overline{OP}_1$ remains finite. Actually this is the case inside the eddies because these turbulent structure are not properly detected by the Smagorinsky operator. A way to avoid such a situation is to scale $\overline{OP}_1$ by $\overline{OP}_2 = (\overline{S}_{ij}\overline{S}_{ij})^{5/2} + (\mathcal{S}_{ij}^d \mathcal{S}_{ij}^d)^{5/4}$. The second term in $\overline{OP}_2$ is negligible near a wall but it avoids numerical instabilities because $\overline{OP}_2$ does not go to zero for pure shear or (ir)rotational strain. Finally, the Wall-Adapting Local Eddy-viscosity model we propose for the eddy-viscosity reads as:

$$\nu_t = (C_w \Delta)^2 \frac{\overline{OP}_1}{\overline{OP}_2} = (C_w \Delta)^2 \frac{\left(\mathcal{S}_{ij}^d \mathcal{S}_{ij}^d\right)^{3/2}}{\left(\overline{S}_{ij}\overline{S}_{ij}\right)^{5/2} + \left(\mathcal{S}_{ij}^d \mathcal{S}_{ij}^d\right)^{5/4}}, \tag{13}$$

where C_w is a (true) constant. A simple way to determine this constant is to assume that the new model gives the same ensemble-average subgrid kinetic energy dissipation as the classical Smagorinsky model. Thus one obtains:

$$C_w^2 = C_s^2 \frac{\left\langle \sqrt{2}\left(\overline{S}_{ij}\overline{S}_{ij}\right)^{3/2} \right\rangle}{\left\langle \overline{S}_{ij}\overline{S}_{ij}\, \overline{OP}_1/\overline{OP}_2 \right\rangle}.$$

C_w can be assessed numerically using several fields of homogeneous isotropic turbulence. The values obtained for six fields are given in table 1. The fields (a) and (b) (respectively (c) and

(d)) correspond to two de-correlated times of simulation of a 64^3 LES while (e) and (f) result from a 128^3 LES. All these computations have been performed with a 6^{th} order compact scheme [18] and the classical structure function model [4] at infinite molecular Reynolds number. From table 1, a value of C_w in the range $0.55 \leq C_w \leq 0.60$ is appropriate for $C_s = 0.18$. A more accurate estimation of C_w is given in the following section.

3 Results

Both subgrid scale models presented in section 2 have been implemented in a computer code based on the *COUPL* (Cerfacs and Oxford University Parallel Library) software library that has been developed at CERFACS and Oxford University [19] . This library uses cell-vertex finite-volume techniques based on arbitrary unstructured and hybrid grids to solve the three-dimensional compressible Navier-Stokes equations. In the present study, we make use of the Lax-Wendroff scheme to advance the conservative quantities. Since the pressure and velocity components are stored at the same nodes, the solution for pressure may not be physical due to even-odd decoupling. Thus a fourth-order artificial viscosity term is added to the density and pressure residuals to damp any node-to-node oscillations that may develop. Note that *no* dissipation is added explicitly to the residuals of the three velocity components. Consequently, the subgrid scale model effects are not corrupted by those of artificial dissipation. This approach has already been successfully used to perform both DNS and LES [20, 14, 15] and is used here to compute turbulent pipe flow. Before conducting such computation, a highly accurate spectral code was used to test the WALE model for the case of decaying isotropic homogeneous turbulence.

3.1 Isotropic Turbulence

We first validate the behaviour of the WALE model for the simple case of a freely decaying isotropic homogeneous turbulence. The experiment by Comte-Bellot & Corrsin [21] on decaying turbulence behind a grid is simulated. In this experiment, the spectra are measured at three downstream locations and the Taylor microscale Reynolds number is in the range 71.6-60.6. In

a reference frame moving with the average flow velocity the problem can be thought of as freely decaying isotropic turbulence. We model this by considering the fluid to be inside a cubical box with periodic boundary conditions [12, 22]. A Galerkin method based on Fourier expansions is applied in all spatial directions. The nonlinear terms are evaluated in the physical space via a pseudo-spectral method; the 3/2-rule is used to eliminate the aliasing errors. The time approximation is achieved with an explicit (low-storage) Runge-Kutta scheme of third order. For more details on the numerical implementation the reader is referred to Dubois et al. [23]. First, a simulation without subgrid scale model is performed on a grid with 256^3 points in order to generate a turbulent field corresponding to the first measurement location in the experiment. Then, the initial field for the LES is obtained by filtering this solution onto a grid with 32^3 points. Figure 1 shows the energy spectrum at the initial time and two subsequent times computed by using the WALE model together with the experimental data. The three spectra correspond to the physical times 42, 98 and 171 M/U_o, where M and U_o stand for the mesh size and the mean convection velocity in the experiment [21]. The best results were obtained with $C_w \approx 0.5$. This value of C_w is in fairly good agreement with the rough estimation provided in the previous section. The model provides the right amount of dissipation so that the experimental spectra are reproduced. Note that the best value for C_w (in terms of reproducing the experimental spectra) was found to be close to 0.45 for a grid with 48^3 points. This dependence on the grid size is not surprising. It is a feature which is shared by all the models with a constant fixed *a priori* and promotes the derivation of a dynamic version of the WALE model. In the following, the constant C_w is set to 0.5.

3.2 Turbulent Pipe Flow

The unstructured numerical tool described above has been used for the simulation of a turbulent pipe flow of radius R and length $4R$, periodic in the streamwise direction x. The Mach number is about 0.25 and the nominal Reynolds number is $R_b = 10000$, based on the bulk velocity U_b and the pipe diameter. It is $R^+ \simeq 320$ based on the friction velocity and the pipe radius. The large eddy simulations have been performed using a hybrid mesh (see figure 2) with structured hexahedral cells near the wall ($r > 0.7R$) and prisms in the core region ($r < 0.7R$). In the region where hexahedral cells are used, 200 points are used in the θ direction whereas 40 points are needed in the x direction, giving a total of 240000 nodes. In wall units this leads to $\delta_x^+ \simeq 28$, $\delta r^+ \simeq 2.1$ (at the wall) and $R\delta_\theta^+ \simeq 8.8$ (at the wall) in the streamwise, radial and azimuthal direction respectively. The initial condition consists of a Poiseuille flow on which is superimposed white noise ($0.1\% amplitude$) that will trigger the transition through non-linear effects. A source term is added to the Navier-Stokes equations to simulate a pressure gradient corresponding to the fully turbulent state; this term comes from a empirical evaluation and reads:

$$\frac{\partial p}{\partial x} = \frac{\lambda}{2R}\frac{\rho U_b^2}{2} \tag{14}$$

with $\lambda = 0.3164 R_b$ (Schlichting [24]).

More details concerning this configuration can be found elsewhere [15]. In this reference, the same flow was computed using both the classical and the filtered version of the Smagorinsky model. In the present paper, the WALE formulation is used and the results are compared to those obtained by using the two previous models. Figure 3 shows the time evolution of the mean total kinetic energy and of the maximum of vorticity during the calculation. All quantities are scaled using U_b and R. After a short period of energy decrease due to the fact that the white

noise prescribed at $t = 0$ is not physical, instabilities develop slowly up to $t \simeq 75\ R/U_b$, then transition to turbulence occurs. For both the filtered and the WALE model a maximum of kinetic energy and ω_{max} is reached for $t \simeq 90\ R/U_b$. After the transition both computations reach a statistically steady state but the turbulent activity and the total kinetic energy are larger with the WALE model. This point is related to the fact that the mean mass flow rate is better assessed with the WALE formulation (see below). As a test, the solution from the WALE model at $t \simeq 85\ R/U_b$ has been used as an initial condition for a calculation performed with the Smagorinsky model and $C_s \simeq 0.18$ [15]. The result is complete relaminarization of the flow confirming the poor behaviour of the classical formulation without constant adjustment.

During the transition to turbulence, the shape of the mean streamwise velocity profile changes and becomes close to what is observed in a turbulent channel flow. Once the fully turbulent regime has been reached with no further changes in the mean streamwise velocity (i.e. among $t \simeq 300\, R/U_b$), we accumulated statistics over $150\, R/U_b$. Figure 4 shows the different stresses in global coordinates. The computation matches the exact total stress reasonably well, establishing the adequacy of the statistical sample. The mean streamwise velocity obtained with the WALE formulation is plotted in wall units in figure 5, together with the classical laws $u^+ = y^+$ and $u^+ = \frac{1}{\kappa} ln(y^+) + C$. For $y^+ > 30$, our results exhibit the classical logarithmic law almost up to the centerline of the pipe flow, as expected from both the numerical and experimental results of Eggels et al. [17]. For the computation with the WALE model, figure 5 also suggests 0.416 for the Von Karman's constant κ and $C \simeq 5$, which is in the common range for turbulent velocity profiles. Smaller values of the constants are representative of the results with the filtered Smagorinsky formulation ($\kappa = 0.39,\ C \simeq 4.5$). Other statistics are provided in figure 6 which shows the root-mean-square of both the streamwise and the radial velocity. The numerical

results are compared with the available PIV measurements [17] at a lower Reynolds number ($R_b = 5450$). The location and the level of the maximum of the turbulence intensity in the streamwise direction are well predicted by the computations. The WALE model produces a level of radial fluctuations slightly lower, which is in better agreement with the experimental data.

An important feature of the WALE model is that it theoretically exhibits the proper near-wall scaling for the subgrid scale eddy-viscosity ($\nu_t = O(y^3)$ if the wall corresponds to $y = 0$). As can been seen in figure 7, this scaling is well reproduced in the performed computation since ν_t is of order r^3 near the pipe wall. The eddy-viscosity is two orders of magnitude smaller than the molecular viscosity in the sublayer so that the small discrepancy from the r^3 behaviour could most likely not have a measurable effect on the results. The curves in figure 7 for the classical and the filtered Smagorinsky formulations have been obtained by applying the corresponding operators to a turbulent field obtained with the WALE model. Clearly both these approaches produce a large amount of eddy-viscosity at the wall. For the former model, this leads to a complete laminarization of the flow. For the latter, the wrong behaviour at the wall reduces the effective Reynolds number of the simulation so that only 85 % of the expected [2] mass flow rate in the pipe was obtained. The effective Reynolds number in this computation is of order 8500. On the other hand, the correct bulk velocity has been reached with the WALE formulation and the effective Reynolds number is close to its nominal value (10000). Note also from figure 7 that the three models lead to similar eddy-viscosity in the core region of the pipe, where the turbulence is nearly isotropic.

[2] The computed mass flow rate (or bulk velocity) can be directly compared to the value provided by the empirical relation used to define the driven source term.

Different visualizations of instantaneous 3D fields have been also performed. Noticeably, the expected elongated turbulence structure can be observed in figure 8 which shows the near wall motion through two iso-surfaces of streamwise velocity. Fig 9 exhibits evidences of turbulent motions at very small scales near the wall, which are well captured by the mesh and the eddy viscosity model. In the core region of the pipe, the turbulence develops at a greater scale (not shown), thus justifying the use of larger prismatic cells near the centerline.

4 Conclusion

A new subgrid scale model based on the square of the velocity gradient tensor is proposed with the following advantages compared to the classical Smagorinsky formulation:

- the spatial operator consists of a mixing of both the local strain and rotation rates. Thus all the turbulence structures relevant for the kinetic energy dissipation are detected by the model,
- the eddy-viscosity goes naturally to zero in the vicinity of a wall so that neither (dynamic) constant adjustment nor damping function are needed to compute wall bounded flows,
- the model produces zero eddy viscosity in case of a pure shear. Thus it is able to reproduce the laminar to turbulent transition process through the growth of linear unstable modes.

Moreover, the WALE model is invariant to any coordinate translation or rotation and only *local* information (no test-filtering operation, no knowledge of the closest points in the grid) are needed so that it is well-suited for LES in complex geometries. From the retained scaling for the spatial operator, the model is numerically well-conditioned: the eddy-viscosity can neither be negative nor infinite. Its efficiency has been demonstrated by computing a freely decaying isotropic turbulence as well as a turbulent pipe flow using a hybrid mesh. All the expected features were observed (natural transition to turbulence, near-wall scaling) and the obtained statistics compare well with the available data.

The WALE model appears to be promising but needs to be tested in more complex cases to assess its potential for different types of flow. Obviously, the pure shear case in which the eddy-viscosity is exactly zero may be seen as a high-Reynolds number limiting case for all the laminar/turbulent shear flows (boundary layers, shear layers, jets) and the model should still be

able to handle transition for such cases. In the case of a laminar flow with a more complex 3D velocity gradient, there is no evidence that the WALE model (or any other SGS model) will give a reasonable answer. The proper asymptotic behaviour of the eddy-viscosity has been clearly shown for the case of a solid wall. As yet, there is no evidence that the WALE model can produce good results in the case of a free surface or a transpiring wall. Also, the generalization of this model to compressible flows in non-trivial. However, the proposed approach is more practical than the dynamic Smagorinsky model since it does not require filtering at various scales. Its implementation in any existing code is straightforward and the overhead is only a few percents.

Acknowledgments

The authors thank Dr. T. Schönfeld and Dr. J.D. Müller for their support on computing aspects. They are also grateful to Prof. J. Hunt for his helpful comments on a draft of this manuscript. All the computations have been performed on the CRAY T3D of CERFACS.

References

[1] Lilly, D.K. A proposed modification of the germano subgrid-scale closure method. *Physics of Fluids*, A4(3):633–635, 1992.

[2] Wray, A.A. and Hunt, J.C.R. Algorithms for classification of turbulent structures. *Topological Fluid Mechanics, Proceedings of the IUTAM Symposium*, pages 95–104, 1989.

[3] Metais, O. and Lesieur, M. Spectral large-eddy simulation of isotropic and stably stratified turbulence. *J. of Fluid Mech.*, 239:157–194, 1992.

[4] Lesieur, M. and Métais, O. New trends in large-eddy simulations of turbulence. *Annual Rev. Fluid Mech.*, 28:45–82, 1996.

[5] Lund, T.S. and Novikov, E.A. Parameterization of subgrid-scale stress by the velocity gradient tensor. *Center for Turbulence Research, Annual Research Briefs*, pages 27–43, 1992.

[6] Van Driest, E.R. On turbulent flow near a wall. *J. of Aero. Sci.*, 23:1007–1011, 1956.

[7] Moin, P. and Kim, J. Numerical investigation of turbulent channel flow. *J. of Fluid Mech.*, 118:341, 1982.

[8] Comte, P., Ducros, F., Silvestrini, J., David, E., Lamballais, E., Métais, O., and Lesieur, M. Simulation des grandes échelles d'écoulements transitionne ls. *AGARD Conference proceedings 551*, pages 14–1/14–11, 1994.

[9] Ducros, F., Comte, P., and Lesieur, M. Large-eddy simulation of transition to turbulence in a boundary layer spatially developing over a flat plate. *J. of Fluid Mech.*, 326:1–36, 1996.

[10] Germano, M., Piomelli, U., Moin, P., and Cabot, W.H. A dynamic subgrid-scale eddy viscosity model. *Physics of Fluids, A*, 3(7):1760–1765, 1991.

[11] Meneveau, C., Lund, T., and Cabot, W. A lagrangian dynamic subgrid-scale model of turbulence. *J. of Fluid Mech.*, 319:353–385, 1996.

[12] Ghosal, S., Lund, T., Moin, P., and Akselvoll, K. A dynamic localization model for large-eddy simulation of turbulent flows. *J. of Fluid Mech.*, 286:229–255, 1995.

[13] Jansen, K. Unstructured-grid large-eddy simulation of flow over an airfoi l. *Center for Turbulence Research, Annual Research Briefs*, pages 161–173, 1994.

[14] Nicoud, F., Ducros, F., and Schönfeld, T. Towards direct and large eddy simulations of compressible flows in complex geometries. *Notes in Numerical Fluid Mechanics, R.Friedrich, P.Bontoux (Eds.).*, 64, 1998.

[15] Ducros, F., Nicoud, F., and Schönfeld, T. Large-eddy simulation of compressible flows on hybrid meshes. *Eleventh Symposium on Turbulent Shear Flows, Grenoble, France*, 3:28–1,28–6, 1997.

[16] Schönfeld, T. and Rudgyard, M. A cell-vertex approach to local mesh refinement for 3d euler equations. *AIAA Paper 94-0318*, 1994.

[17] Eggels, J.G.M., Unger, F., Weiss, M.H., Westerweel, J., Adrian, R.J., Friedrich, R., and Nieuwstadt, F.T.M. Fully developed turbulent pipe flow: a comparison between dire ct numerical simulation and experiment. *J. of Fluid Mech.*, 268:175–209, 1994.

[18] Lele K.S. Compact finite difference schemes with spectral-like resolutio n. *J. of Comp. Physics*, 103:16–42, 1992.

[19] Rudgyard, M., Schönfeld, T., Struijs, R., and Audemar, G. A modular approach for computational fluid dynamics. *Proceedings of the 2nd ECCOMAS–Conference,Stuttgart*, 1994. Also exists as CERFACS Technical Report TR/CFD/95/07.

[20] Nicoud, F.C., Poinsot, T.J., and Ha Minh, H. Direct numerical simulation of turbulent flow with massive uniform injection. *Tenth Symposium on Turbulent Shear Flows, The Pennsylvania State University*, 1995.

[21] Comte-Bellot, G. and Corrsin, S. Simple eulerian time correlation of full- and narrow-band velocity signals in grid generated, 'isotropic' turbulence. *J. of Fluid Mech.*, 48:273–337, 1971.

[22] Moin, P., Squires, K., Cabot, W., and Lee, S. A dynamic subgrid-scale model for compressible turbulence and scalar transport. *Physics of Fluids, A*, 3(11):2746–2757, 1991.

[23] Dubois, T., Jauberteau, F., and Temam, R. Incremental unknowns, multilevel methods and the numerical simulation of turbulence. *Comput. Methods Appl. Mech. and Engrg.*, 159:123–189, 1998.

[24] Schlichting, H. Boundary layer theory. *Mc-Graw Hill publisher*, 1979.

List of Tables

List of Figures

	Field a	Field b	Field c	Field d	Field e	Field f
α	10.81	10.52	10.84	10.55	10.70	11.27

Table 1: Values of C_w^2/C_s^2 from different turbulent fields.

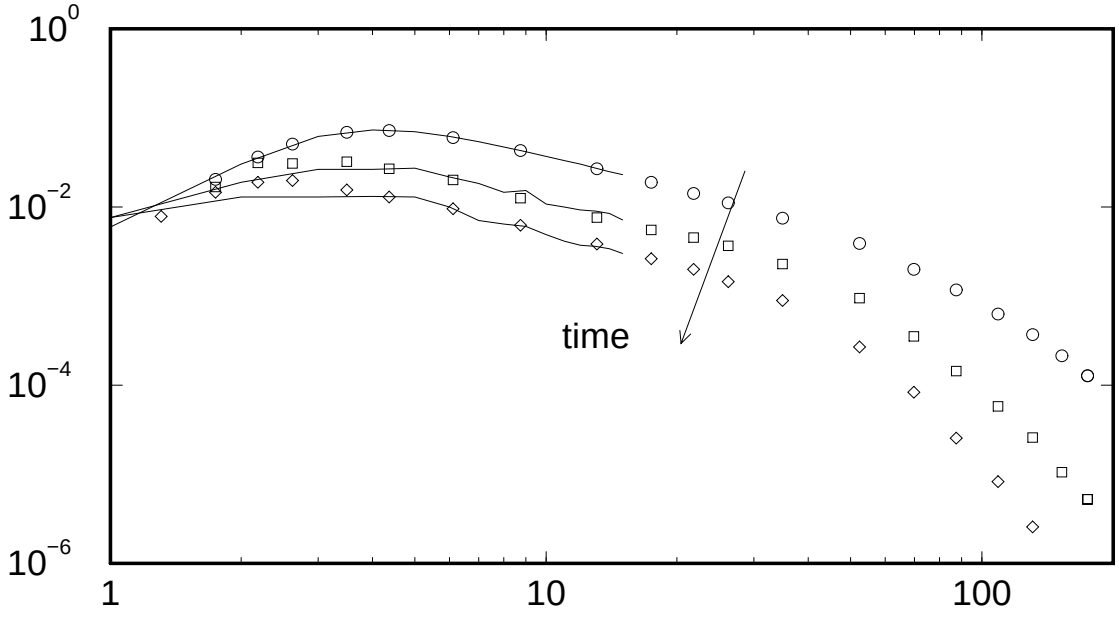

Figure 1: Time evolution of energy spectra for freely decaying isotropic turbulence with the WALE model. The grid contains 32^3 points. Symbols are experimental mesurements. Times are 42, 98 and 171 M/U_o

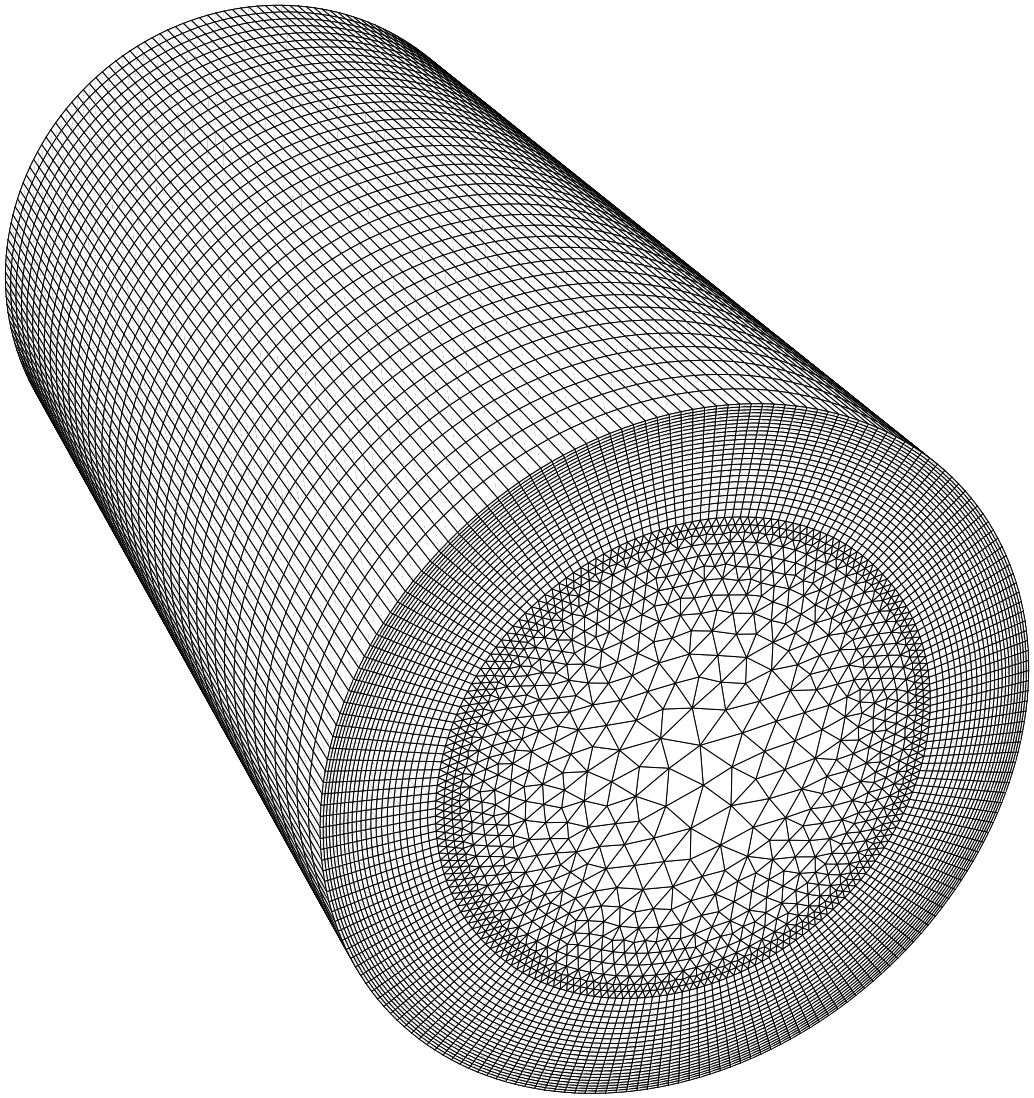

Figure 2: The hybrid grid used for the LES of a turbulent pipe flow.

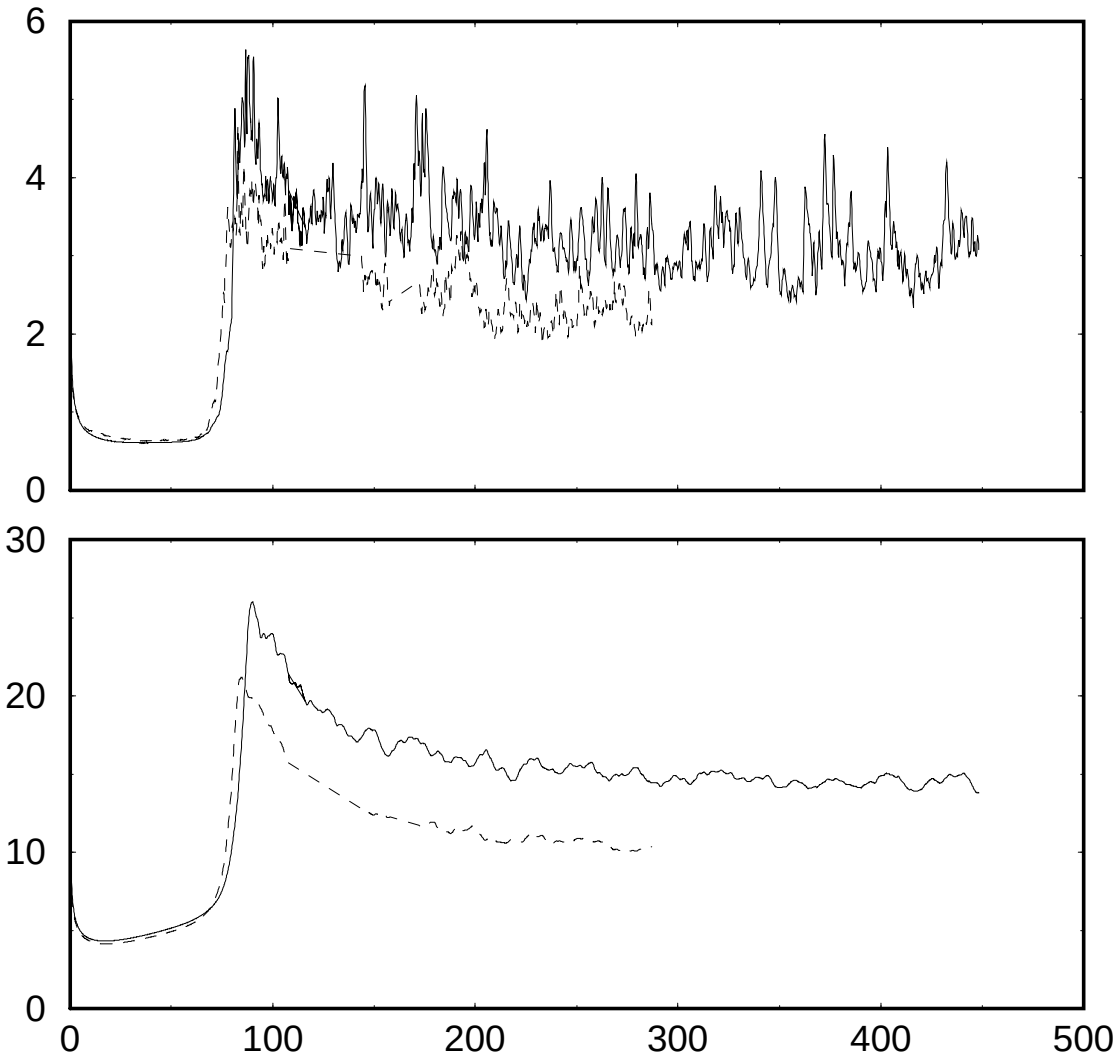

Figure 3: Time evolution of kinetic energy (bottom) and of maximum of vorticity (top) with both the filtered-Smagorinsky (– – –) and the WALE (——-) models. Time unit is R/U_b

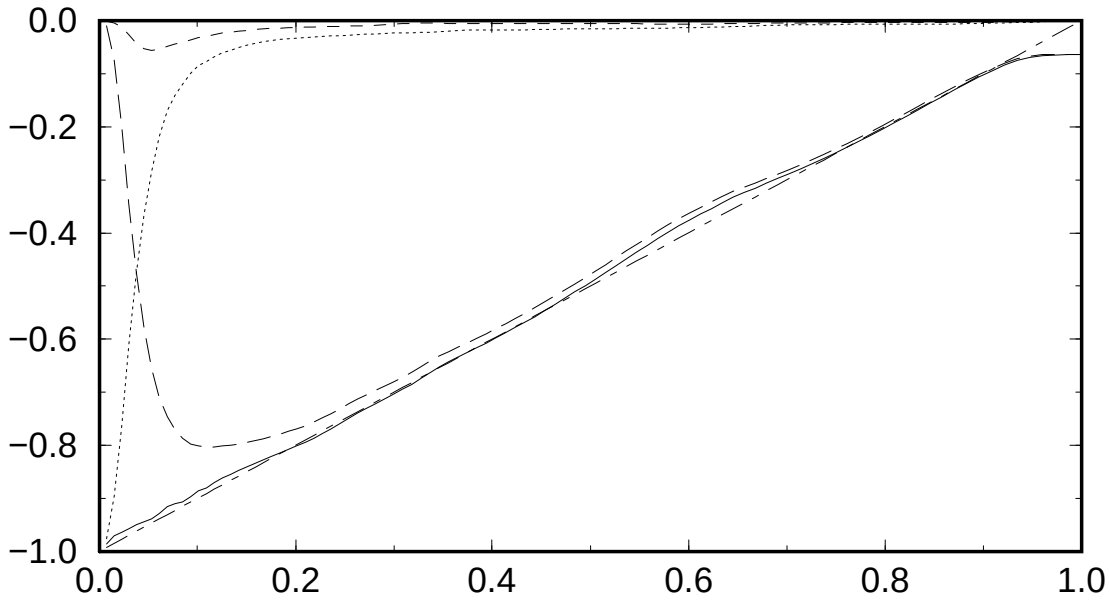

Figure 4: Resolved stress (– – –), subgrid stress (- - - -), subgrid and viscous stress (.....) and total computed stress (——) distributions, normalized by the wall shear stress, vs. the distance to the wall. The exact total stress is denoted by the dot-dashed line.

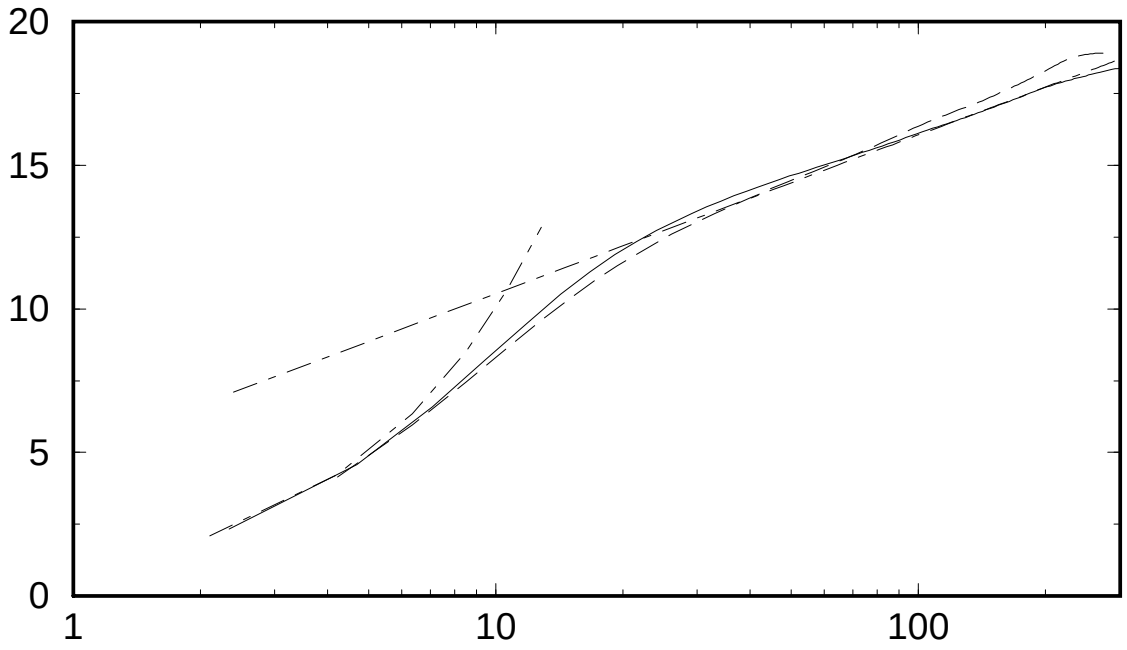

Figure 5: Mean velocity profile vs. the distance to the wall (semi-log coordinates). Comparison between the filtered-Smagorinsky model (– – –) and the WALE formulation (——). The law-of-the-wall is denoted by the dot-dashed line.

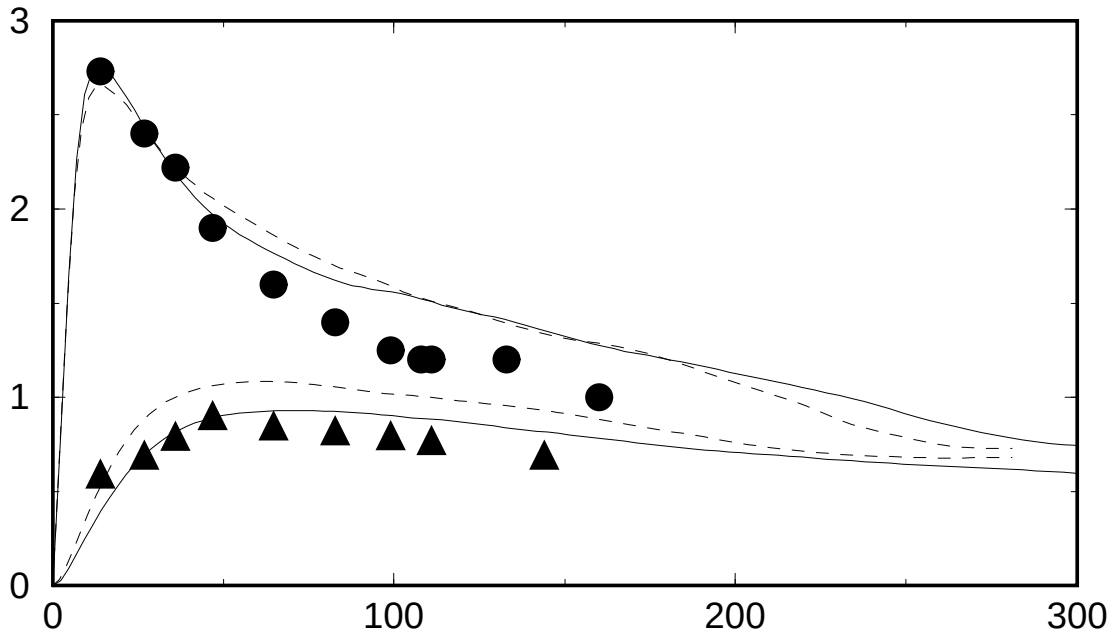

Figure 6: Root-mean-square streamwise velocity and normal velocity vs. the distance to the wall. Comparison between the filtered-Smagorinsky model (– – –) and the WALE formulation (——). The experimental data from Eggels et al. for $R_b = 5450$ is denoted by symbol.

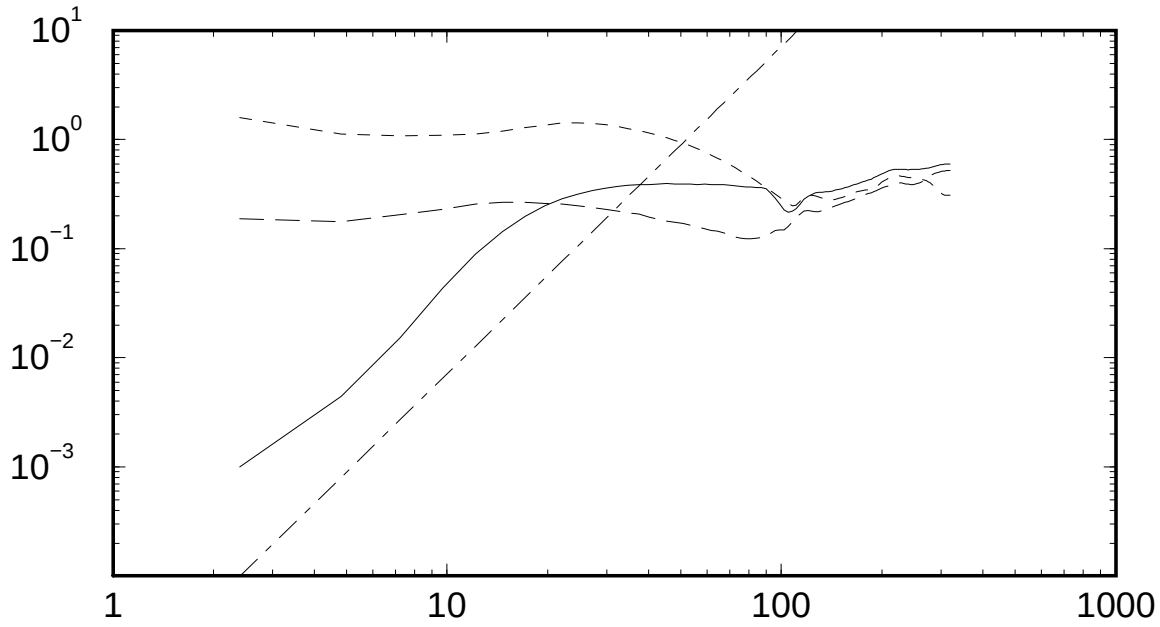

Figure 7: Ratio of average eddy-viscosity to molecular viscosity vs. the distance to the wall (log-log coordinates). Comparison between the classical Smagorinsky model (- - - -), its filtered version (– – –) and the WALE model (——). The proper near-wall scaling is denoted by the dot-dashed line.

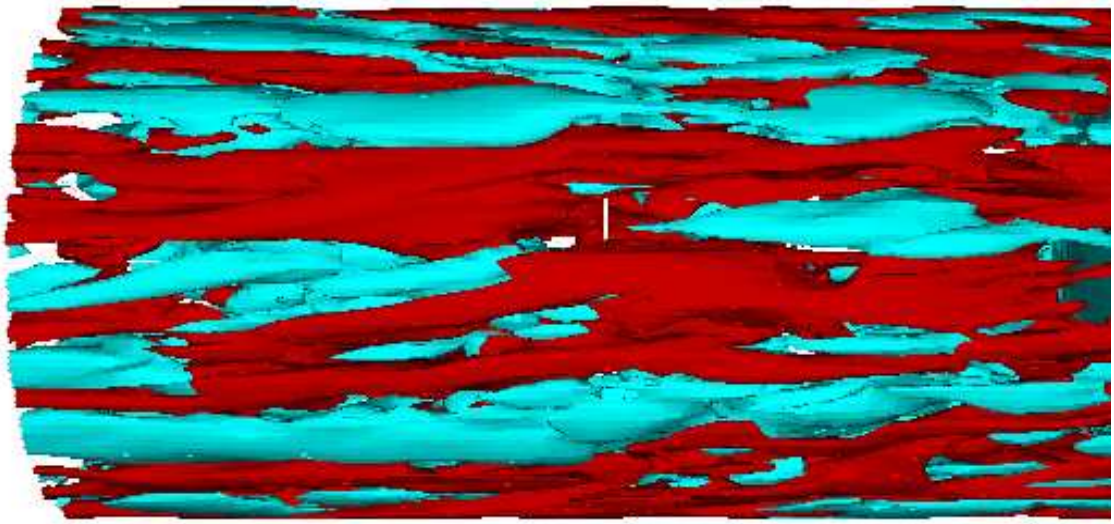

Figure 8: WALE computation. Iso-surface $u' = -0.1U_c$ (black) and $u' = +0.1U_c$ (grey).

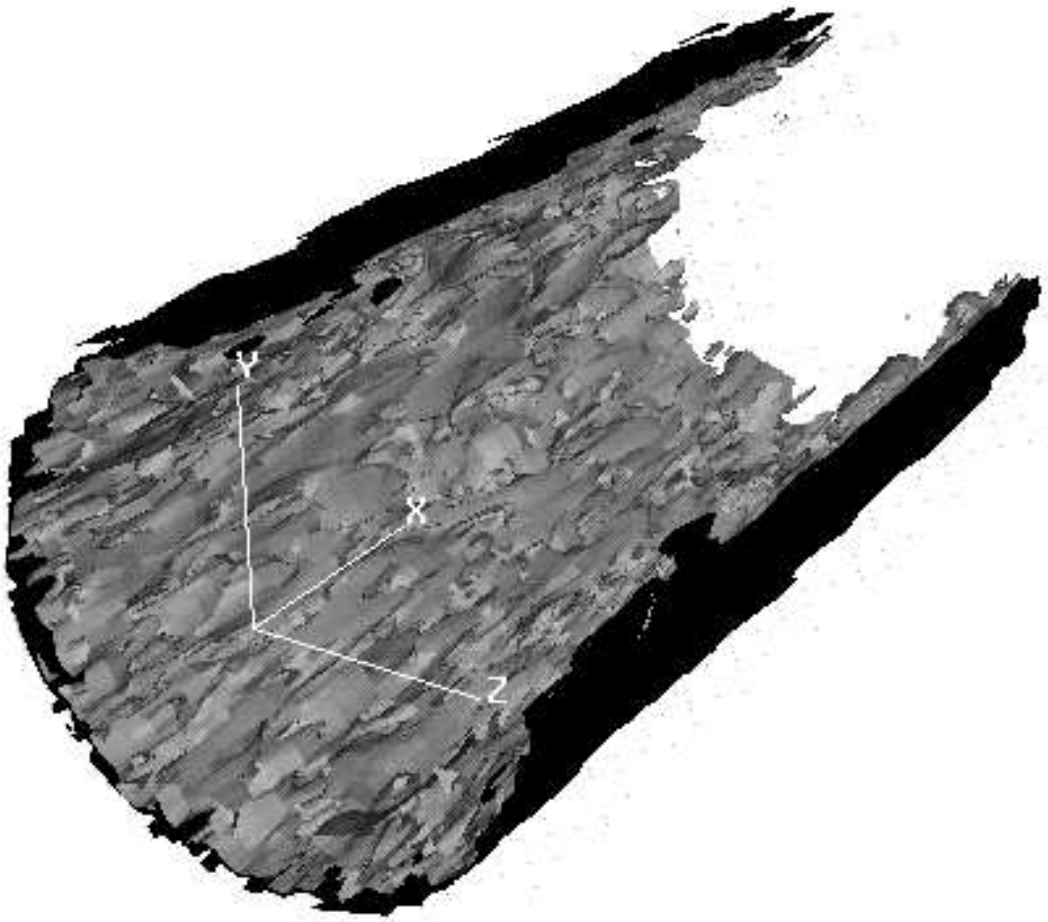

Figure 9: WALE computation. Iso-surface $(\omega^2)^{1/2} = 3U_b/R$ (black) and $(\omega^2)^{1/2} = 7U_b/R$ (grey).